Modeling of reflectance properties of ZnO film using artificial neural networks

A. G. YUKSEK[a], E. SENADIM TUZEMEN[b], S. ELAGOZ[c]
[a]*Department of Computer Engineering, Cumhuriyet University, 58140 Sivas, Turkey*
[b]*Nanophotonics Center, Department of Physics, Cumhuriyet University, 58140 Sivas, Turkey*
[c]*Nanophotonics Center, Department of Nanotechnology Engineering, Cumhuriyet University, 58140 Sivas, Turkey*

A ZnO thin film was prepared on a p-Si (100) substrate by using a pulsed filtered cathodic vacuum arc deposition system (PFCVAD). Specular reflectance, a nondestructive technique, can be used to measure thickness, refractive index of thin films grown on reflecting substrate and their dependancy on reflecting angle. In this study, the effects of reflectance angle on specular reflectance measurements of ZnO thin film is modeled by Artificial Neural Networks (ANN) utilizing " Multi-Layer Perceptron (MLP)", Back propagation Algorithms Levenberg Marqued that is learning rule on incident angle range of 30-60 degrees. Also it is shown that reliable high precision measurements can be obtained without using expensive high precision hardware.

(Received January 20, 2015; accepted October 28, 2015)

Keywords: ZnO thin film, Artificial neural networks, Reflectance

1. Introduction

Zinc oxide is a wide and direct-bandgap semiconductor with an energy gap of 3.37 eV at 300 K [1]. High transmission properties in visible range and with an excitation binding energy up to 60 meV makes it one of the promising candidate for fabricating surface acoustic wave instruments, gas sensors, solar cells and heat reflecting windows [2,3,4]. When Si technology is experienced, the output is inexpensive, abundant and easy to manufacture. This alone makes ZnO thin film growths on Si an important area of research [5] for several applications such as n-ZnO/p-Si hetero junction photo diodes [4,6].

Spectroscopic measurements of thin films are very important. It is a nondestructive technique and enables us to gather important film parameters such as refractive index, thin film layer thickness and their dependency to incident angle. The angle dependent measurements are tedious experimental processes and the precise increment of the incident angle is important to develop a reliable model.

In this paper, the effect of incident angle dependency of reflection data from ZnO thin film grown on Si substrate is modeled by Artificial Neural Networks (ANN) utilizing "Multi-Layer Perceptron (MLP)", Back propagation (BP) Algorithms Levenberg Marqued (LM) learning rule for 30°, 45° and 60° for a wavelength range from 200 nm – 2400 nm. The refined model was then used to generate reflectance spectra for an untrained incident angle (50°) and was confirmed with experiment.

ZnO thin films modeled using the artificial neural networks have been studied by some researchers. Kim et al. [7] studied Ga-doped zinc oxide (ZnO:Ga) thin films which were prepared on glass substrate by magnetron sputtering. They have been analyzed and modeled by using the artificial neural networks (NNets) for the effects of film thickness and annealing temperature on sheet resistance, transmittance and figure of merit of ZnO:Ga thin films. They showed that the NNet models present the good prediction on sheet resistance, transmittance and figure of merit of ZnO:Ga thin films. Genetic algorithm (GA) has been used to search the optimized recipe for the desired figure of merit of ZnO:Ga thin films. Co et al. [8] investigated by using ANN based on radial basis function networks (RBFN) and multi-layer perceptron (MLP) of ZnO thin films grown by pulsed laser deposition (PLD). They used two input parameters and a response parameter. Photoluminescence (PL), which is one of the main parameters to determine the optical characteristic of the structure. In order to minimize the joint confidence region of fabrication process with varying the conditions, D-optimal experimental design technique was performed and PL intensity was characterized by neural networks. Finally, they used statistical methods to verify the fitness of nonlinear process models. Co et al. [9] studied ZnO films which were deposited with varying substrate temperature in the range of 350–450°C and oxygen pressure in the range of 250–450 mTorr. They investigated the process by modeling the growth rate in pulsed laser deposition (PLD)-grown ZnO thin films and used ANN based on the back-propagation (BP) algorithm and the process recipes were optimized via genetic algorithms (GAs) in their study. Solookinejada et al. [10] studied the zinc oxide (ZnO) thin film which was fabricated by sol–gel spin coating method. They applied Genetic

Algorithm (GA) for characterization and extracting the physical parameters of the film. X-ray reflectivity (XRR) and its optimization were used in GA. Kim et al. [11] studied the effects of deposition process parameters on deposition rate and electrical properties of In_2O_3–10wt% ZnO (IZO) thin films which were modeled and analyzed by using the error back-propagation neural networks (BPNN). In this study, established BPNN model explained the mechanism of IZO deposition process. The deposition rate of IZO thin films is affected by RF power and substrate temperature. Nijnatten [12] studied to discuss the use of variable angle spectrophotometry (VAS) for determining the thickness and optical constants of multi-layer coatings with materials such as ZnO, Cr, ITO and SiO_2.

2. Experimental

2.1 Sample preparation

ZnO thin films were grown on Si (100) substrate by pulsed filtered cathodic vacuum arc deposition. In this study, the substrate temperature was kept constant at room temperature during growth. The base pressure of the deposition chamber was ~10^{-5} Torr and the working pressure was ~3.33×10^{-2} Torr. The base pressure and working pressures were controlled by SRS Stanford Research Systems Model PPM 100. High purity (99.999 % pure) oxygen were introduced into the chamber and controlled by multi gas controller. ZnO thin films were grown using metallic target (Zn, 99.99 %, 1 mm in diameter). After ZnO thin films were deposited by PFCVAD process, the specular reflectance of the ZnO thin films on Si substrate were measured by using a double-beam UV–Vis–NIR spectrophotometer with a Cary 5000.

2.2 Reflectance measurement

Specular reflectance of the ZnO thin film was measured at a wavelength range of 200–2400 nm, using a double-beam UV–Vis–NIR spectrophotometer with a Cary 5000. We had two apparatus called ERA30 and ERA60 (Harrick Scientific's Specular Reflection Accessory) which were able to measure 30° and 60°. In order to improve database impacts on the AAN model, the database should be as possible as much to be able to represent the nature of the problem. Therefore, new apparatus which is able to measure 30°, 45°, 50° and 60° were designed and built according to the original apparatus and then reflectivity measurements were taken by using mirror assemble (Model No: MOP-116, Dimensions: 50x50x3.2 mm UV-Vis Reference & Mirror). Validation of the results of measurements were made with home-made apparatus and then were compared with the measurements made by the original apparatus (30°, 60°) and as aresult, identical reflection spectrums were observed.

2.3 Modeling of artificial neural networks

2.3.1 Artificial Neural Networks (ANN)

An ANN is a computer based mathematical representation of human brain and tries to simulate its learning abilities. ANNs are computational tools which were found wide utilization in solving variety of complex real-world problems due to their remarkable information processing characteristics such as nonlinearity, high parallelism, fault and noise tolerance, and learning and generalization capabilities [13-16]. ANN is an information processing paradigm and the key element of this paradigm is composed of a large number of highly interconnected processing elements (artificial neurons Fig. 1) working in harmony to solve specific problems.

The artificial neuron given in Fig. 1 has 'n' input, denoted as x_1, x_2...x_n. Each line connecting these inputs to the neuron, a weight which is denoted as w_1, w_2... w_n respectively, is assigned to the neuron. The weights in the artificial model correspond to the synaptic connections in biological neurons. The threshold in artificial neuron is usually represented by θ and the activation corresponding to the graded potential is given by the Eq. (1): [17]

$$a = \left(\sum_{j=1}^{n} w_j x_j\right) + \theta \;\rightarrow\; O_j = f(a) \qquad (1)$$

ANNs have been studied and explored by many researchers and have been applied and manipulated in almost every field, the examples include system identification and modeling and prediction and classification [13]. The Back propagation neural network is a multilayered, feed forward perceptron neural network simplest and most general methods were used for supervised training of multilayered neural networks. Back propagation operates by approximating the non-linear relationship between the input and the output by adjusting the weight values internally. It can further be generalized for the input that is not included in the training patterns.

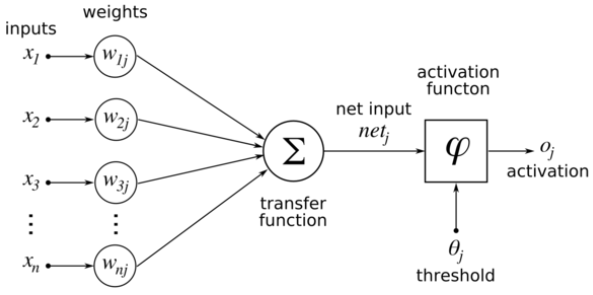

Fig. 1. Schematics of a mathematical model of an artificial neuron

2.3.2 Multi-layer feed forward artificial neural networks (MLP)

In MLP Networks neurons and layers are designed in feed forward manner. The first layer is the input layer

where the data set about the problem desired to be solved are received. The last layer is the output layer that data manipulated in the network is obtained. Fig. 2 shows the topology of the Multi-Layer Feed Forward Perceptron (MLP) neural network that includes the input layer, one hidden layer and an output layer. It should be noted that MLP neural networks can have more than one hidden layer. Technically, the main purpose of ANN is to determine the black box model which represents the structure of sample data set. For doing this, network is made to generalize by training with samples of the case [18]. During the training process, input training sets or examples are presented to the input layer of a network. The activation values of the input nodes are weighted and accumulated at each node in the hidden layer [19]. The main purpose behind the most supervised learning rules is the updating of the ANN weights and the bias terms, until the mean-squared-error (Eq (2.2)) between the output predicted by the network and the desired output are less than tolerance [20].

$$e_i(n) = d_i(n) - y_i(n) \tag{2.1}$$

$$E(n) = \frac{1}{N}\sum_{n=1}^{N}\left(\frac{1}{2}\sum_{i=c} e_i^2(n)\right) \tag{2.2}$$

The weights and bias terms are updated and adjusted based on the comparison of the output and the target, until the network output matches the target with calculated error terms by using back propagation algorithm [17]. In Fig. 3, the graphic representation of MLP learning is given. Once the ANN is trained properly, then it can be used to take any decision in the application. Neural networks are adjusted, or trained, so that a particular input leads to a specific target output [21]. Typically, many such input/target pairs are needed to train a network.

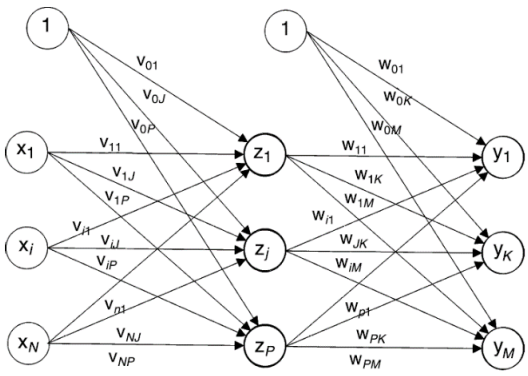

Fig. 2. Multi-Layer Perceptron Neural Network.

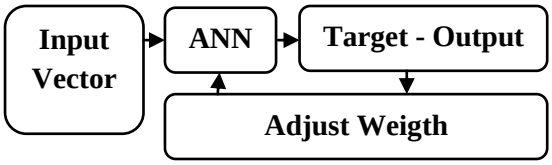

Fig. 3. A learning Cycle in the ANN model

2.3.3 Levenberg–Marquardt Training

Levenberg-Marquardt back propagation training algorithm was used to train all MLP models in this work. The Levenberg–Marquardt algorithm [22,23], which was independently developed by Kenneth Levenberg and Donald Marquardt, provides a numerical solution to the problem of minimizing a nonlinear function. It is fast and has consistent convergence. In the ANN based solutions, this algorithm is suitable for training not very large sized problems [24].

In order to make sure that the approximated Hessian matrix $\boldsymbol{J^TJ}$ is invertible, Levenberg–Marquardt algorithm was planned to approach second-order training speed without having to compute the Hessian matrix. When the performance function has the form of a sum of squares (as is typical in training feed forward networks), then the Hessian matrix can be approximated as

$$H \cong J^T \mu T \tag{3.1}$$

where $\boldsymbol{\mu}$ is always positive, called combination coefficient $\boldsymbol{I}$ is the identity matrix [25].

From Eq. (3.1), one may notice that the elements on the main diagonal of the approximated Hessian matrix will be larger than zero. The update rule of Levenberg–Marquardt algorithm can be presented as

$$w_{k+1} = w_k - \left(J_k^T J_k + \mu I\right)^{-1} J_k e_k \tag{3.2}$$

As the combination of the steepest descent algorithm and the Gauss–Newton algorithm, the Levenberg–Marquardt algorithm switches between the two algorithms during the training process.

2.4 Preparing Data Set and Constructing ANN Model

Preparing data is serious process in neural network modeling for data analysis and it has a profound effect on the success of data analysis, such as data mining and knowledge discovery [26]. The main reason is that the quality of the input data into neural network models may strongly influence the results of the data analysis [27]. As can be seen from Fig. 4, neural network modeling for complex data analysis has four main processes: problem identification, data preparation, neural network modeling, and data analysis. In the first process, problem definitions and expected results are formulated to guide the subsequent tasks. The aim of the second process, data preparation, is to prepare high-quality data for data analysis so as to obtain satisfactory results. In the third process, after initialization, neural network models are trained iteratively. Finally, depending on the generalized results, the goal of the complex data analysis, such as data mining and decision support, can be realized [11].

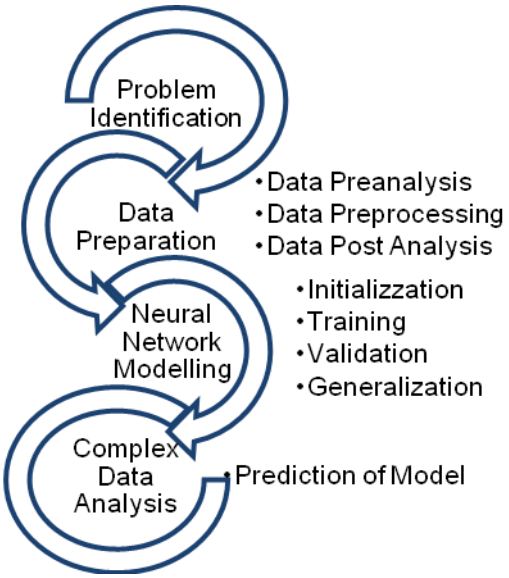

Fig. 4. The process of neural network data analysis.

Database which was used in this study, as seen Table 1, consists of two independent (input) variables and one dependent (output) variable and was obtained with experimental studies.

Table 1 Dependent and Independent Variables.

Independent Variables	
The wavelength (nanometer)	X_1
The angle of incident (degree)	X_2
Dependent Variable	
Reflectance %R	Y_1

The realized measurements (Fig. 5) were obtained by changing the angle between incident light plane and normal (30, 45, 50, 60), in order to determine the reflection behavior of the beam according to wavelength of reflected light as seen Fig. 6.

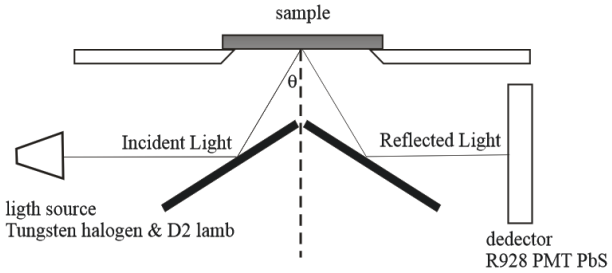

Fig. 5. Optical design of accessory

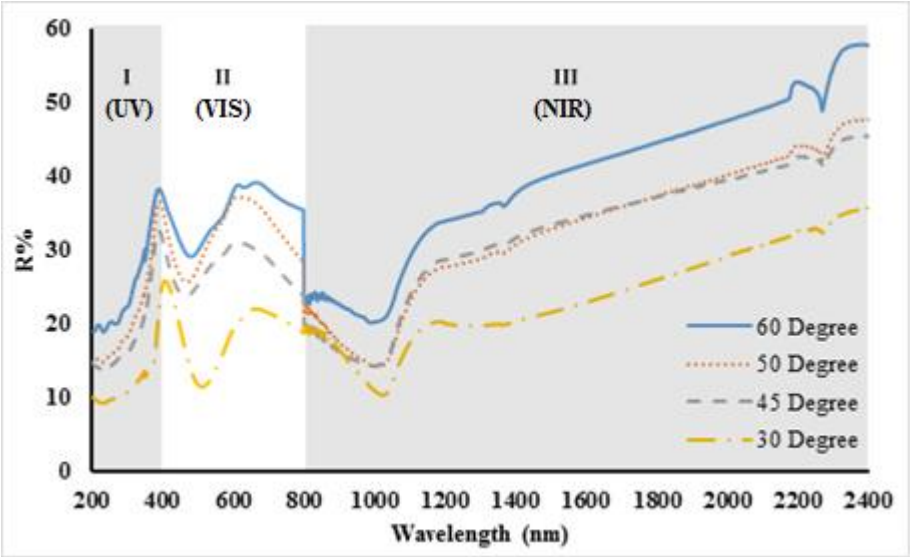

Fig. 6. 200-2400 nm (Data Set) wavelength measurements

As mentioned before, measurements were made in different incident angles between 200 -2400 nm wavelengths with Cary 5000. Cary 5000 using different hardware configurations (different detectors and light sources) in UV (Ultraviolet) region, in visible region and in NIR (Infrared) region.

In order to remove unwanted experimental measurement mishaps, which result from the configuration change of the hardware device (different light sources in different wavelength regions), results obtained from the measurements have been evaluated by the ANN model separating three groups depicted in Fig. 7 and Table 2, separately. Each groups were submitted to ANN models to train and construct their structures.

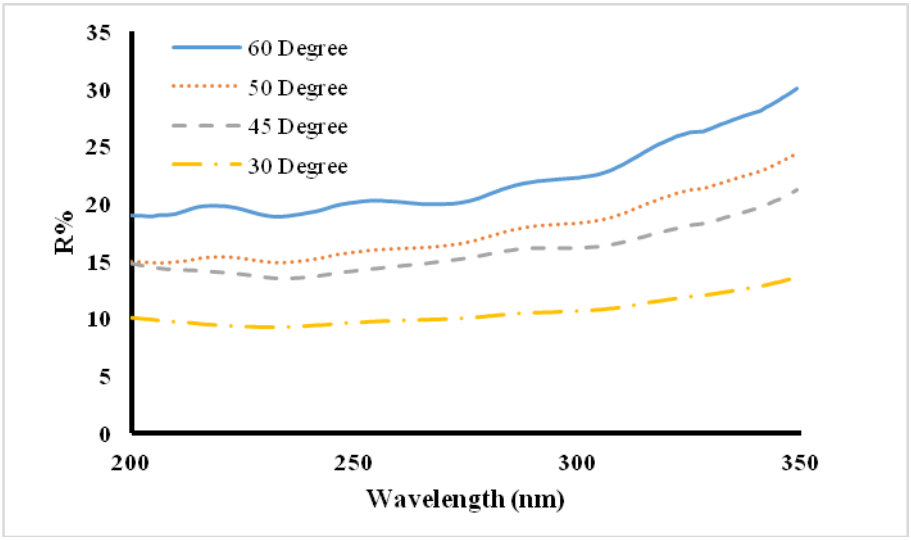

(a)

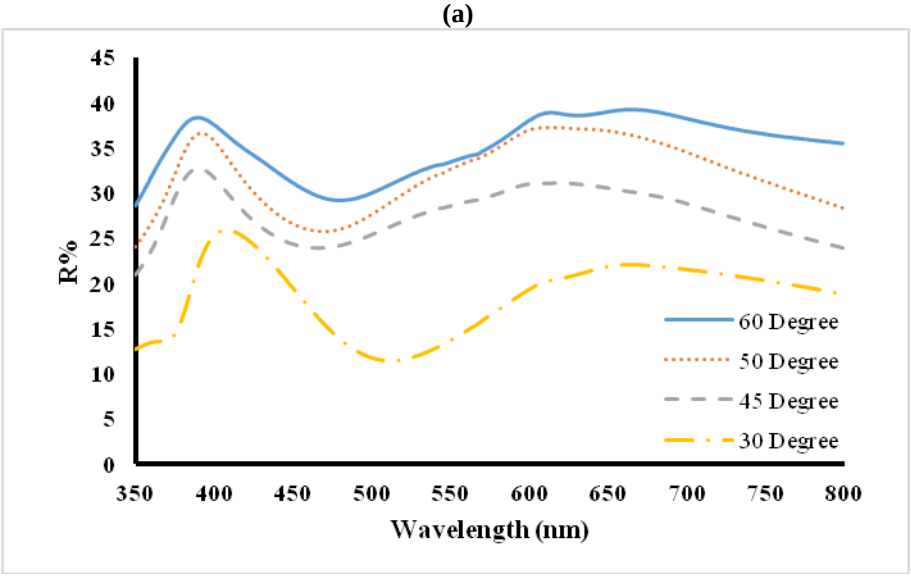

(b)

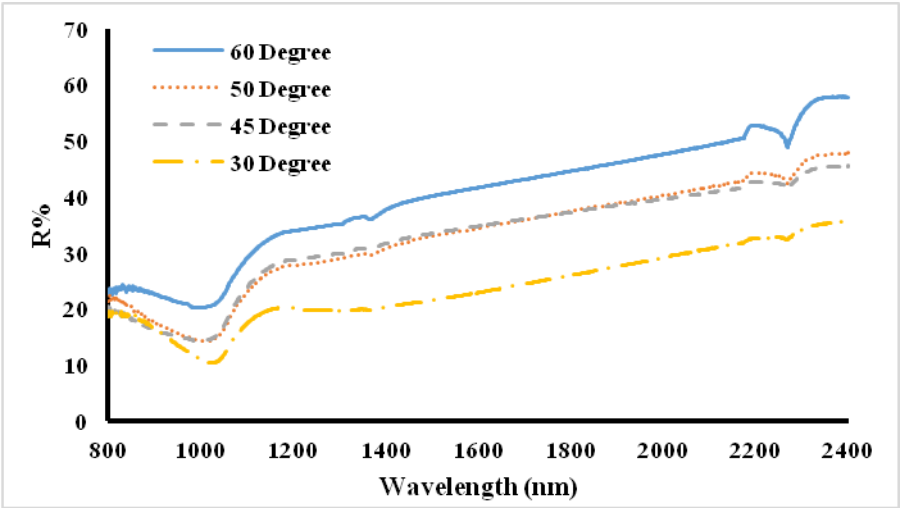

(c)

Fig. 7. (a) 200 - 350 nm (Data Set 1) wavelength measurements (UV region). (b) 350 -800 nm (Data Set 2) wavelength measurements (VIS region), (c) 800 -2400 nm (Data Set 3) wavelength measurements (NIR region)

Table 2 Separation of Data Sets.

I (UV)	200nm-350nm	30^o, 45^o and 60^o	Data Set 1 Training set
	200nm-350nm	50^o	Data Set 1 Control set
II (VIS)	350nm-800nm	30^o, 45^o and 60^o	Data Set 2 Training set
	350nm-800nm	50^o	Data Set 2 Control set
III (NIR)	800nm-2400nm	30^o, 45^o and 60^o	Data Set 3 Training set
	800nm-2400nm	50^o	Data Set 3 Control set

The other critical process is the development of the ANN model. The fundamental aim of the development part is determination of training parameters, hidden layer numbers and neuron numbers in each layer. With the training of determined model, the values of the connections between each neurons are calculated. This is known as the architecture of ANN model. The ANN architecture directly depends on complexity of problems to be solved and the design steps of this architecture based on experience. Therefore, the expert has to test several experiments using different architecture parameters in order to generate best ANN model.

4. Results and discussion

4.1 Determining Reflectance Angle With Neural Networks

The main objective of the neural network learning which is known as a function optimization problem is to determine the best network parameters in order to minimize the network error. Determination steps of ANN architecture and parameters were made as follows and can be seen in Fig. 8:

- Database were constituted based on the measurements which were made with 30^o, 45^o and 60^o degree apparatus (accepted as training data set Table 2). After that, database were separated into three parts according to wavelength (200 - 350 nm (Data Set 1), 350 - 800 nm (Data Set 2) and 800 - 2400 nm (Data Set 3)).
- The sequential data sets were submitted to ANN architecture that were constituted presumptively according to experience and similar models in literature, and training of ANN for each part were started.
- In order to validate to the determined ANN architecture (accepted as controlling data set as seen Table 2), we generated data for 50° and compared it with the measurements which were made with 50° apparatus.
- The best model (ANN architecture and parameters) giving the best result for the discussed problem was determined by MSE (Mean Squared Error), MAPE (Mean Absolute Percent Error) and R^2 (Correlation Coefficient*)* values.

MSE (Mean Squared Error): In statistics, the mean squared error (MSE) of an estimator is one of the many ways to quantify the difference between values implied by an estimator and the true values of the quantity being estimated. MSE measures the average of the squares of the "errors." The error is the amount by which the value implied by the estimator differs from the quantity to be estimated.

MAPE (Mean Absolute Percent Error) : MAPE is the most common measure of forecast error. MAPE functions were best when there are no extremes in the data (including zeros). With zeros or near-zeros, MAPE can give a distorted picture of error. The error on a near-zero item can be infinitely high, causing a distortion to the overall error rate when it is averaged in.

R *(Correlation Coefficient*): A correlation coefficient is a statistical measure of the degree to which changes to the value of one variable predict change to the value of another.

ANN models that were used during trials produced very convenient results in most of the trials with training datasets (Table 2), but it should be decided that which one is the best. Training databases for the best final ANN architecture are the starting point for the determination of the parameters. For each of training sets, ANN model trained with initial parameters that are determined with experience and similar studies in literature. At the end of each trial MSE, MAPE and R^2 values are calculated. The MSE value should be convergent to zero and the MAPE value should be smaller as possible, respectively. But R value is preferred to be ≤ 1 and cannot be greater than 1. If these values are not in acceptable range then ANN model retrained with new input parameters such as hidden layer numbers, neuron numbers in each layer, etc. When the calculated parameters for studied model are appropriate, then this model is used for validation. After determination of ANN architecture, “Control Datasets (Table 2)” which were never used in training ANN model are submitted to studied model and this model generates MSE, MAPE and R^2 values. If these values are within the acceptable range, this model is considered as final model and the training is finished. Table 3 shows the values of decision parameters and ANN architecture model is obtained from the trials.

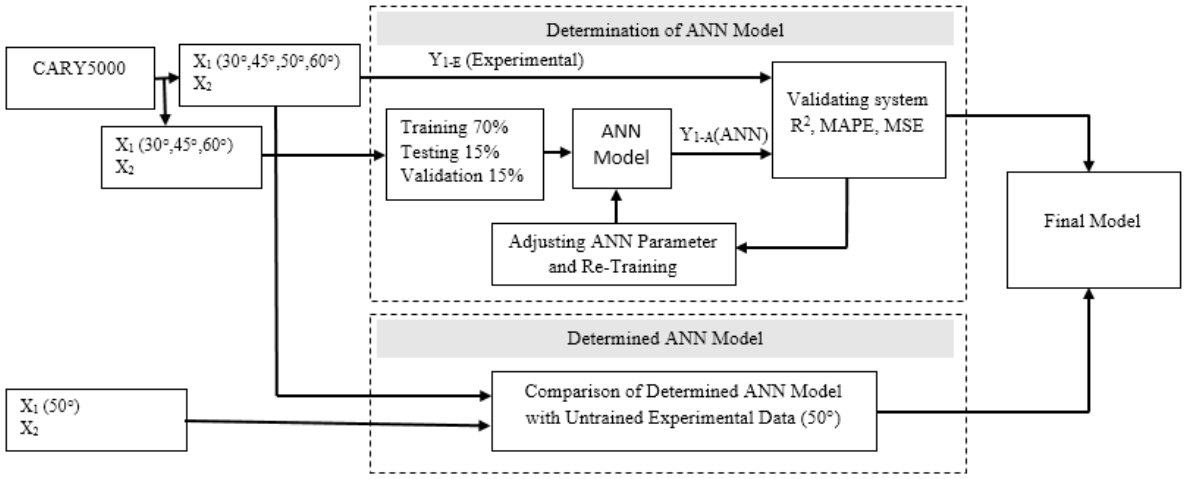

Fig. 8. Block Diagram of Determination ANN Model

Table 3 ANN Architectures used in modelling.

	200 - 350nm	**350 - 800nm**	**800 - 2400nm**
Number of input layer	**1**		
Number of hidden layer	**3**		
Number of output layer	**1**		
Layer map	**2-6-8**	**2-6-8**	**3-6-8**
Performance function	**MSE**		
Train function	**Levenberg-Marquardt**		
Learning rate	**0.5**	**0.5**	**0.5**
Momentum coefficient	**0.8**	**0.8**	**0.8**

The comparison of the observed and measured values according to Dataset 1 – Training Set is shown in Fig. 9. As can be seen clearly from Fig. 8 and Table 4, the established model (Table 3) represents the nature of this problem in best manner with training dataset. Comparison results of validation can be seen in Fig. 10. The Fig. 11 represents the behavior of ANN model results according to Dataset 1 Control set and the measured values. In the light of trials results, it is shown that the nature of problem in UV region is represented well by generated ANN model for Dataset 1.

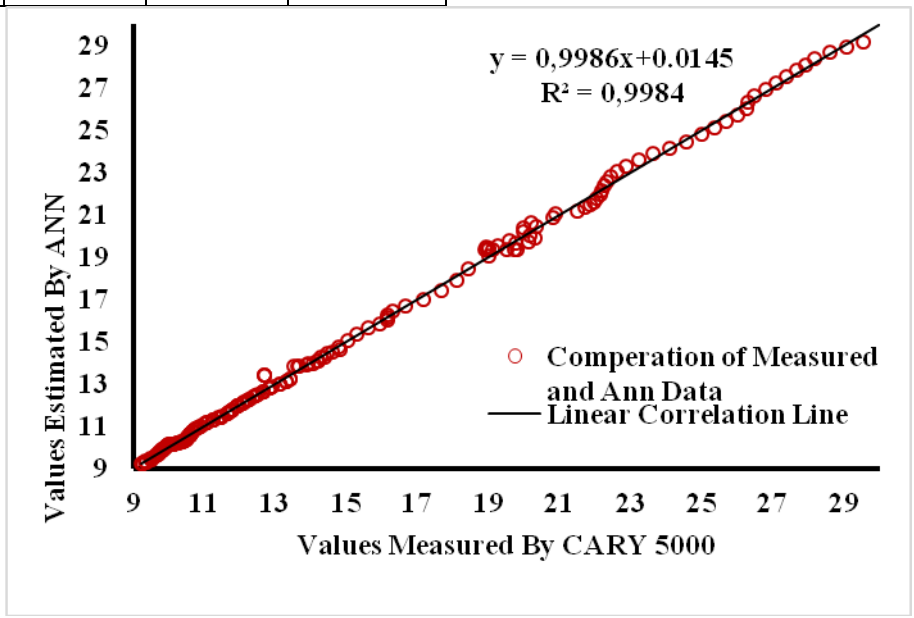

Fig. 9. Comparison of Measured and Estimated Values with Dataset (Dataset 1-Training Set, UV)

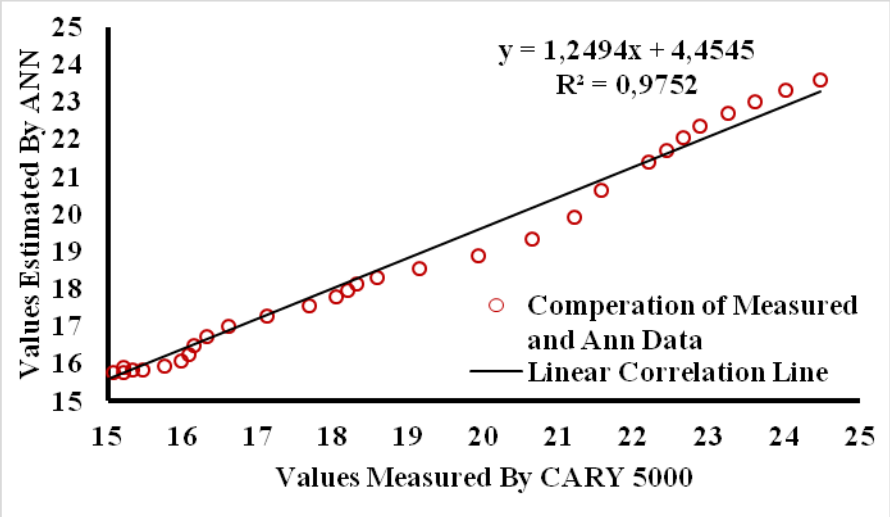

Fig.10. Relation of Measured and Estimated Values with Dataset (Dataset 1-Control Set, UV)

The next step is the determination of ANN model for the visible wavelength region. To determine the ANN model, dataset 2 was submitted to the produced ANN model by Dataset 1. The wondering point here is, whether the determined ANN model by Dataset 1 represents same behavior with Dataset 2 or not. The graph which can be seen in Fig. 12 gives the answer to this question. Dataset 2 Training Set produced very good results in ANN model. Fig. 13 and Fig. 14 show the validation of this model with Dataset 2 Validation Set and the success of ANN model is proven by those Figures.

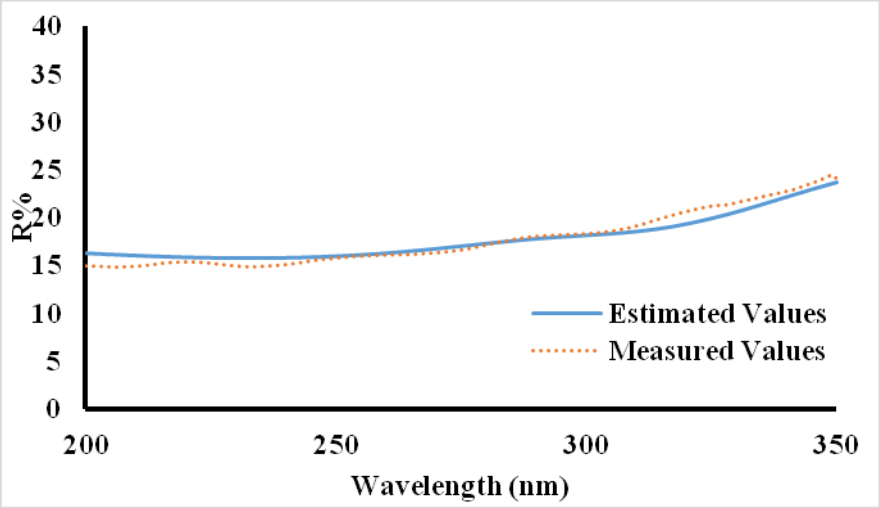

Fig. 11. Comparison of Measured and Estimated Values with Dataset (Dataset 1- Control Set, UV)

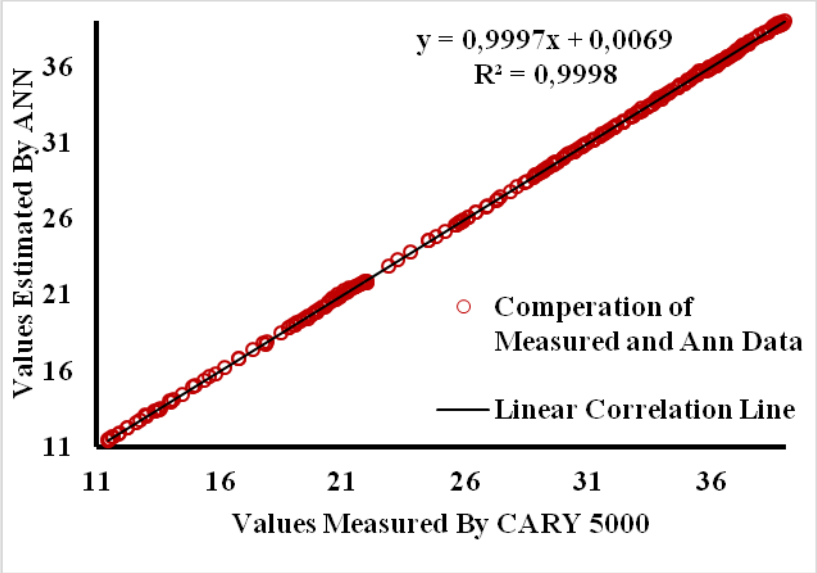

Fig. 12. Comparison of Measured and Estimated Values with Dataset (Dataset 2-Training Set, VIS)

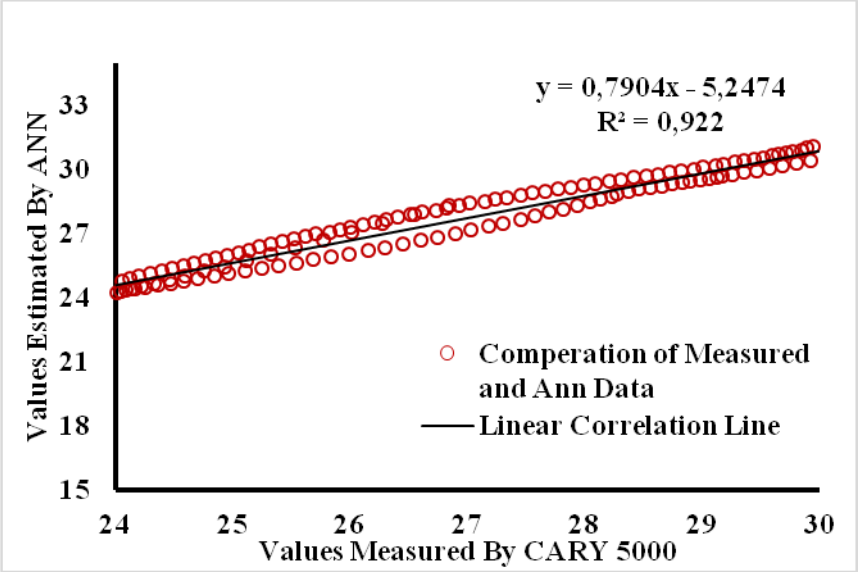

Fig. 13. Relation of Measured and Estimated Values with Dataset (Dataset 2-Control Set, VIS)

In the last section of this study, we tried to obtain ANN models for NIR region. However, due to the physical nature of the problem, the ANN model obtained for Dataset 1 and Dataset 2 could not produce acceptable results for Dataset 3. Therefore a new ANN model is obtained by retraining with new input parameters such as hidden layer numbers, neuron numbers in each layer, etc. When the calculated parameters for the studied model are appropriate, then this model was used for validation. The results of the new adjusted model are shown in Table 3 and Table 4, Fig. 15, Fig. 16 and Fig. 17 for Dataset 3.

Table 4. ANN Models Results.

Data Set		ANN Architecture	MSE	MAPE	R^2
200 - 350 nm (DataSet 1, UV)	Training Set	2-6-8	0.0439	0.8784	0.9984
	50^o Controlling Set	2-6-8	0.4906	3.3353	0.9752
350 – 800 nm (DataSet 2, VIS)	Training Set	2-6-8	0.0038	0.00628	0.9998
	50^o Controlling Set	2-6-8	1.5088	3.5740	0.922
800 – 2400 nm (DataSet 3, NIR)	Training Set	3-6-8	0.0162	2.3667	0.9999
	50^o Controlling Set	3-6-8	5.5671	9.8465	0.9958

The values parameters produced by ANN models are presented in Table 4. Finally the calculated reflectance spectra from 200-2400 nm was plotted (Fig. 18). Comparing Fig. 6 and Fig. 18 which represents the experimental results and the results of the ANN model, it is clear that the constructed models in this study represent the nature of problem in UV-VIS-NIR range.

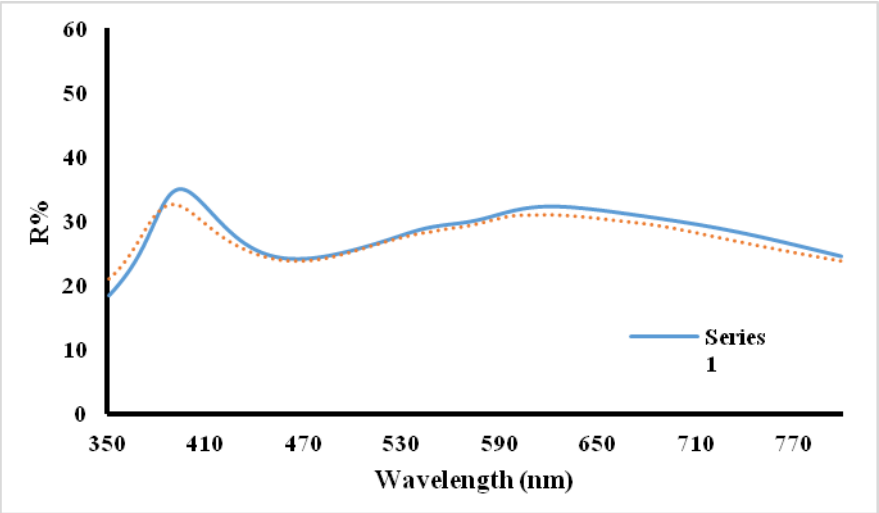

Fig. 14. Comparison of Measured and Estimated Values with Dataset (Dataset 2-Control Set, VIS)

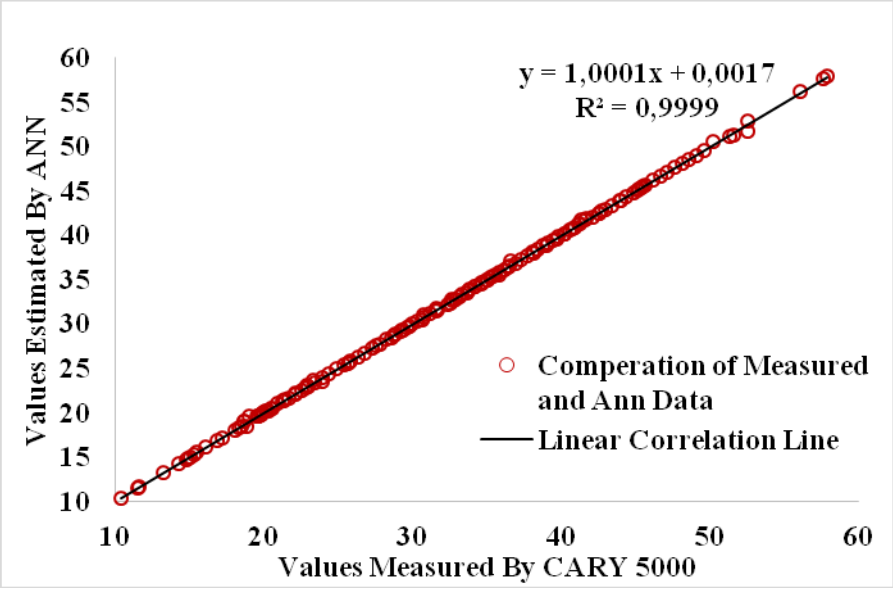

Fig. 15. Comparison of Measured and Estimated Values with Dataset (Dataset 3-Training Set, NIR)

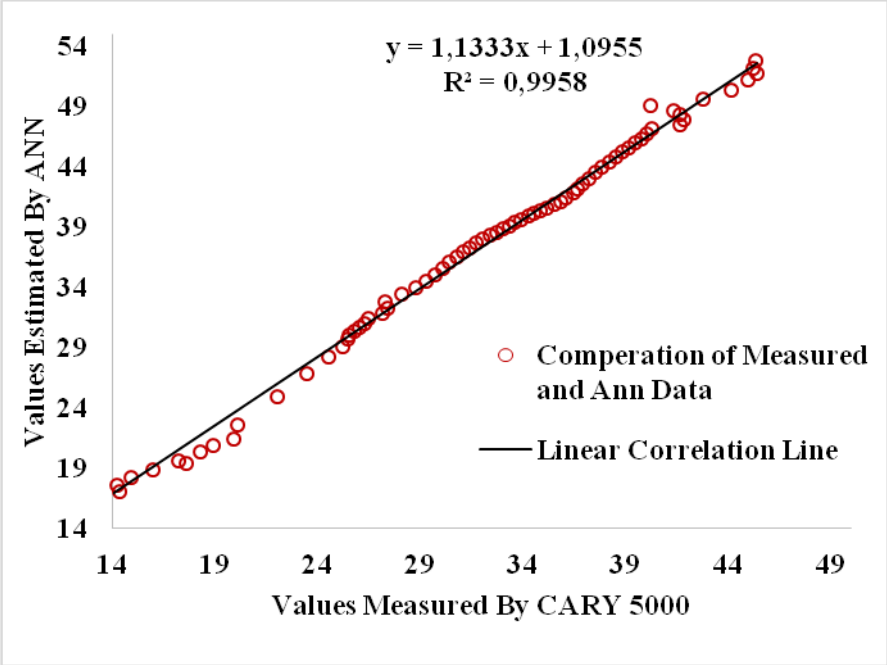

Fig. 16. Relation of Measured and Estimated Values with Dataset (Dataset 3-Training Set, NIR)

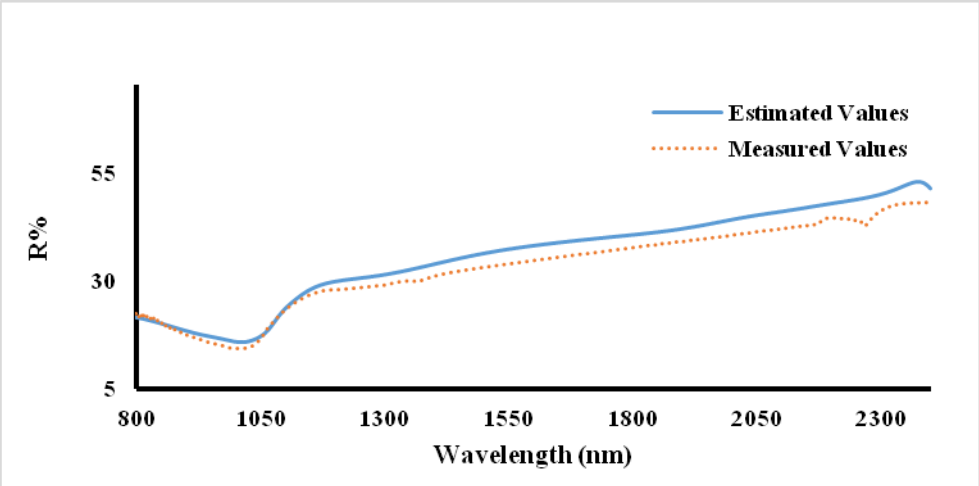

Fig. 17. Comparison of Measured and Estimated Values with Dataset (Dataset 3-Control Set, NIR)

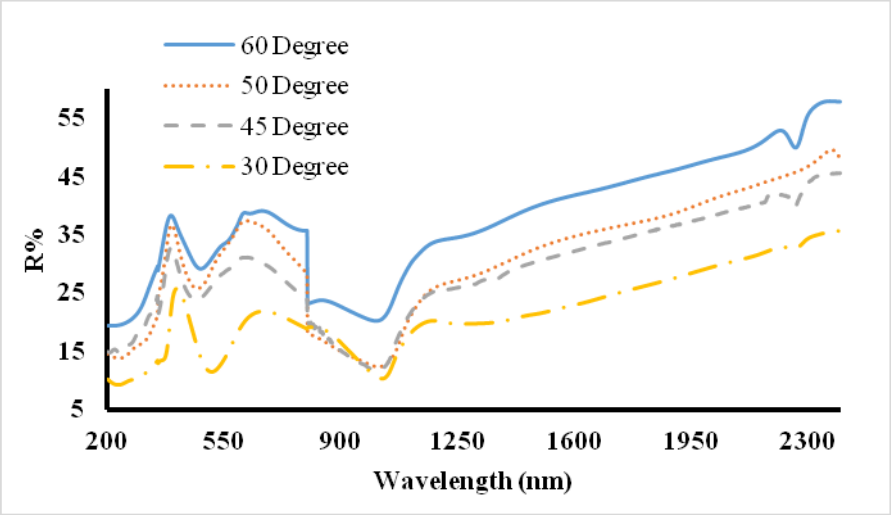

Fig. 18. The results of ANN Models in 200-2400 nm wavelength region

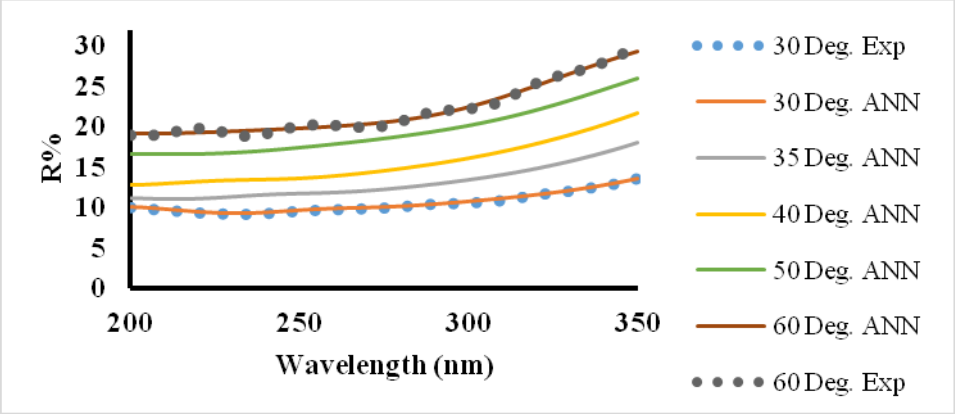

Fig. 19. Compare of 200-350 nm wavelength Experimental Produced and ANN Models Results (UV)

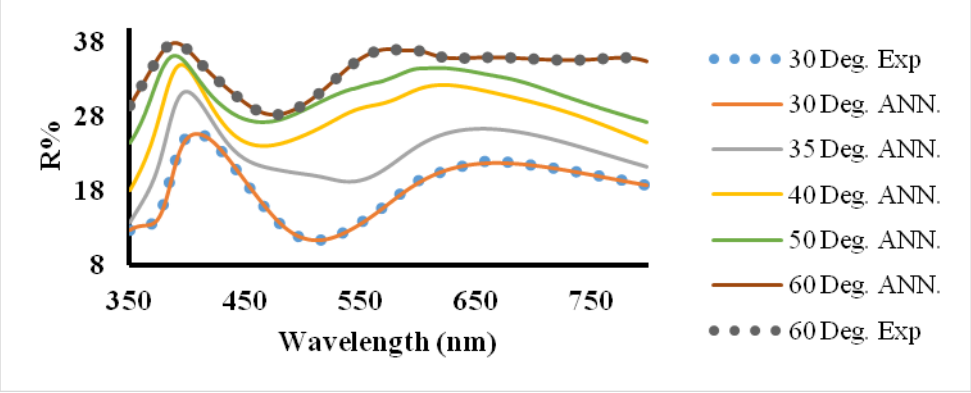

Fig. 20. Compare of 350-800 nm wavelength Experimental Produced and ANN Models Results (VIS)

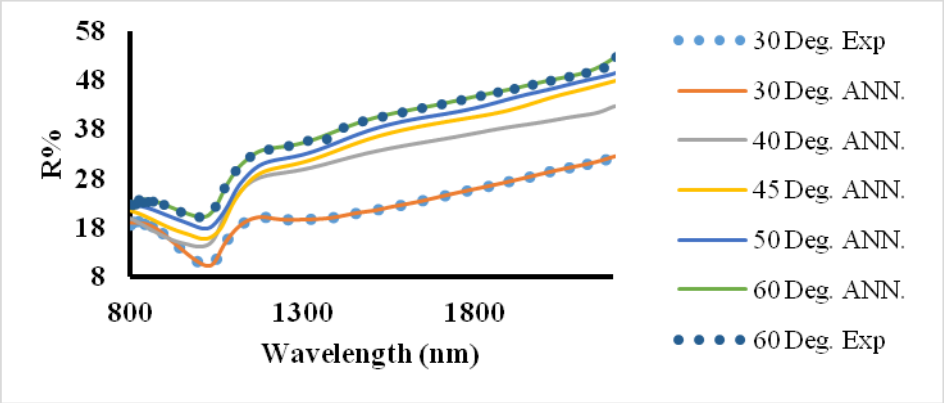

Fig. 21. Compare of 800-2400 nm wavelength Experimental Produced and ANN Models Results (NIR)

As mentioned earlier, it is time consuming to obtain data from experimental work with very little increment of the incoming angle. Also the experimental setup is quite expensive for such measurements. However, we represent a novel way of generating angle dependency by measuring some angles in the region of interest, then using the models generated by ANN architecture obtaining the spectra in between with any precision desired. As an example, we successfully generated data using ANN model in 30°-60° angle covering the full spectrum from 200 - 2400 nm range with increments smaller then experimentally obtainable in our experimental setup. For better comparison we also added some experimentally obtained values for 30° and 60° in Fig. 19, Fig. 20, and Fig. 21. From these figures, it is clear that the trend of ANN models follows the physical nature of the problem.

4. Conclusions

We grew ZnO on p-Si (100) substrate by pulsed filtered cathodic vacuum arc deposition system. We investigated the effects of incident angle on specular reflectance of ZnO thin film which was analyzed and modeled using the experimental data and ANN model. ANN models which have produced the best MSE, MAPE and R^2 values were chosen to generate simulation that can be used to generate the reflection behavior of the incident light beam with different angles of incidence for UV-VIS-NIR regions. It has been shown that the model based on the generated data complies with the experimental data. The results of this study prove that by measuring the reflectance spectra from the incident angle of 15 degrees interval by generating data in 1 degrees (or even better) increment precision by ANN model is possible to produce which not only can save time but also helps to avoid buying expensive high resolution hardware. Similar studies by using this approach to obtain a wide range of optical data with standard laboratory equipment is possible and under progress.

Acknowledgements

This research was supported by Scientific Research Project Fund of Cumhuriyet University under the project number F-382.

References

[1] A. Janotti, C. G. V. Walle, Rep. Prog. Phys., **72**, 126501 (2009).
[2] H. Yamada, Y. Ushimi, M. Takeuchi, Y. Yoshino, T. Makino, S. Arai, Vacuum, **74**, 689 (2004).
[3] K. Tominaga, T. Murayama, I. Mori, T. Okamoto, K. Hiruta, T. Moriga, I. Nakabayashi, Vacuum, **59**, 546 (2000).
[4] H. Qi, Q. Li, C. Wang, L. Zhang, L. Lv, Vacuum, **81**, 943 (2007).
[5] Z. Y. Xiao, Y. C. Liu, D. X. Zhao, J. Y. Zhang, Y. M. Lu, D. Z. Shen, X. W. Fan, Journal of Luminescence, **122–123**, 822 (2007).
[6] J. Y. Lee, Y. S. Choi, W. H. Choi, H. W. Yeom, Y. K. Yoon, J. H. Kim, S. Im, Thin Solid Films, **420 –421**, 112 (2002).
[7] C. E. Kim, P. Moon, I. Yun, S. Kim, J. M. Myoung, H. W. Jang, J. Bang, Expert Systems with Applications, **38**, 2823 (2011).
[8] Y. D. Ko, H. S. Kanga, M. C. Jeong, S. Y. Lee, J. M. Myoung, I. Yun, Journal of Materials Processing Technology, **159**, 159 (2005).
[9] Y. D. Ko, P. Moon, C. E. Kim, M. H. Hamb, J. M. Myoung, I. Yun, Expert Systems with Applications, **36**, 4061 (2009).
[10] G. Solookinejada, A. S. H. Rozatiana, M. H. Habibi, Applied Surface Science, **258**, 260 (2011).
[11] C. E. Kim, H. S. Shin, P. Moon, H. J. Kim, I. Yun, Current Applied Physics, **9**, 1407 (2009).
[12] P.A.V. Nijnatten, Thin Solid Films, **516**, 4553 (2008).
[13] I. A. Basheer, M. Hajmeer, Journal of Microbiological Methods, **43**, 3 (2000).
[14] M. E. Petersen, D. Ridder, H. Handels, Pattern Recognition, **35**, 2279 (2002).

[15] M. Mohanraj, S. Jayaraj, C. Muraleedharan, Renewable and Sustainable Energy Reviews, **16**, 1340 (2012).
[16] C. Baladrón, J. M. Aguiar, L. Calavia, B. Carro, A. S. Esguevillas, L. Hernández, Senors, **12**, 1468 (2012).
[17] L. Fausett, Fundamentals of Neural Networks : Architectures, Algorithms and Applications, (1994).
[18] E. Oztemel, Yapay Sinir Aglari. Istanbul: Papatya Yayincilik, 2003 (in Turkish).
[19] O. Kaynar, I. Yilmaz, F. Demirkoparan, Energy Education Science and Technology Part A: Energy Science and Research, **26**, 221 (2011).
[20] A. G. Parlos, B. Fernandez, A. F. Atiye, J. Muthusami, W. K. Tsai, IEE Transactions on neural networks, **5**, 493 (1994).
[21] D. D. Vishwakarma, International Journal of Advanced Research in Electrical, Electronics and Instrumentation Engineering, **1**, 206 (2012).
[22] K. Levenberg, Quarterly of Applied Mathematics, **2**, 164 (1944).
[23] D. Marquardt, Journal on Applied Mathematics, **11**, 431 (1963).
[24] H. Yu, B. M. Wilamowski, Intelligent Systems Citation Information Edited by J. David Irwin CRC Press, Print ISBN: 978-1-4398-0283-0 (2011).
[25] M. T. Hagan, M. Menhaj, IEEE Transactions on Neural Networks, **5**, 989 (1994).
[26] X. Hu, Applied Mathematics Letters, **16**, 889 (2003).
[27] K. U. Sattler, E. Schallehn, A data Preparation Framework Based on a Multidatabase Language. In: Proc. Int'l Symp. Database Eng. & Applications (2001) 219-228.

*Corresponding author: esenadim@cumhuriyet.edu.tr, ebru_senadim@hotmail.com